

# A New FD Calculus: Simple Grids for Complex Problems

**Abstract** — In the proposed new Finite Difference (FD) calculus of Flexible Local Approximation MEthods (FLAME), the numerical accuracy is qualitatively improved by incorporating any desirable local approximating functions (such as harmonic polynomials, plane waves, cylindrical or spherical harmonics, and so on) into the scheme. While one motivation is to minimize the notorious ‘staircase’ effect at curved and slanted interface boundaries, the new approach has much broader applications and implications. Although the method usually operates on regular Cartesian grids, it is in some cases much more accurate than the Finite Element Method with its complex meshes. The main ideas of FLAME are reviewed and a tutorial-style explanation of its usage is included. As illustrative examples, the paper presents super-high-order three-point schemes for the 1D Schrödinger equation; classical schemes (including the Collatz “Mehrstellen” schemes) as particular cases of FLAME; electrostatic interactions of colloidal particles; scattering; wave propagation in a photonic crystal; plasmon resonances.

Keywords: Generalized Finite Difference Method; Flexible Approximation; Many-Body Interactions; The Schrödinger Equation; The Poisson-Boltzmann Equation; Wave Propagation; Scattering; Photonic Crystals; Plasmon Particles.

## I A PREVIEW

Would it not be wonderful if one could solve geometrically non-trivial problems on simple Cartesian grids with the same accuracy as the Finite Element Method (FEM) provides on complex meshes? Would it not be even better if the Cartesian grid could be much *coarser* than the FE mesh and still yield the same level of accuracy?

This is obviously a tall order, and yet for some interesting and important classes of problems the methods described in this paper do fill the bill. As an alternative, there is a legitimate more conservative question: given a regular geometrically non-conforming grid, what is – in some sense – “the best” one can do?

In the paper, the answer to these questions involves a new Finite Difference (FD) calculus referred to by the acronym ‘FLAME’: Flexible Local Approximation MEthods. The word ‘Flexible’ implies that any desired approximation of the solution (exponentials, spherical harmonics, plane waves, generic or special polynomials, etc.) can be incorporated directly into the FD scheme. The approximation is always treated as *local*, with the intention to represent *local* features of the solution that in many cases may qualitatively be known *a priori* (for example, the behavior of the potential near a material interface).

As a preview, compare two meshes (Fig. 1) that give about the same level of accuracy for a simple 2D test: a cylindrical magnetic particle (with relative permeability  $\mu = 100$ ) immersed in a uniform external field. The FE mesh has 125,665 degrees of freedom (d.o.f.); the relative error in the potential at the nodes is  $2.07 \cdot 10^{-8}$ . The FLAME grid has 900 d.o.f. ( $30 \times 30$ ), and the relative error in the potential at the nodes is  $2.77 \cdot 10^{-8}$  if 9-point ( $3 \times 3$ ) stencils are used. This type of problem will be considered in more detail in Section VI.I.

The paper contains, in a condensed and revised form, part of

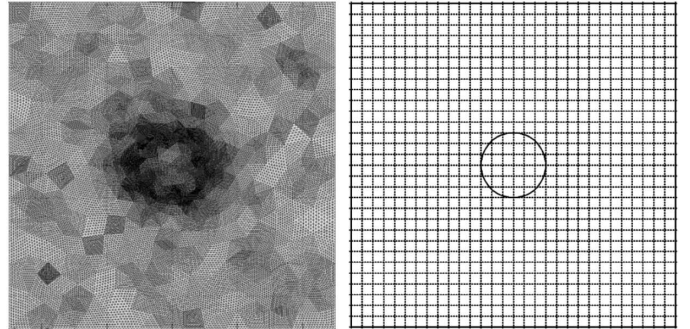


Figure 1: Two meshes yielding about the same level of accuracy for the particle problem. The FE mesh has 31,537 nodes, 62,592 second order triangular elements and 125,665 degrees of freedom. The FLAME grid has 900 degrees of freedom.

the material that will appear in [93], [94].

## II INTRODUCTION: COMPUTATIONAL METHODS WITH FLEXIBLE APPROXIMATION

In many electromagnetic problems some salient features of the solution are qualitatively known *a priori*. Such features include singularities at point sources, edge and corners; boundary layers; derivative jumps at material interfaces; strong dipole field components near polarized spherical particles; electrostatic double layers around colloidal particles – and countless other examples. Such “special” behavior of physical fields is arguably a rule rather than an exception. Clearly, taking this behavior into account in numerical simulation will tend to produce more accurate and physically meaningful results.

One motivation for developing a new class of methods is to minimize the notorious ‘staircase’ effect at curved and slanted interface boundaries on regular Cartesian grids. In the spirit of “Flexible Local Approximation”, the behavior of the solution at the interfaces is represented *algebraically*, by suitable basis functions on simple grids, rather than *geometrically* on conforming meshes. More specifically, fields around spherical particles can be approximated by several spherical harmonics; fields scattered from cylinders – by Bessel functions, and so on. Such analytical approximations are incorporated directly into the difference scheme.

One salient example of the utility of the new approach is problems with multiple moving particles, such as for example in magnetically driven assembly [102], [103]. Indeed, generation of geometrically conforming FE meshes is obviously quite complicated or impractical when the particles move and their number is large (say, on the order of a hundred or more). Standard FD schemes would require unreasonably fine meshes to resolve the shapes of all particles. Parallel adaptive Generalized FEM has been developed [37], [38], [39], but the procedure is quite complicated both algorithmically and computationally. The celebrated Fast Multipole Method (FMM) has clear advantages for systems with a large number of known charges or dipoles in free

space (or a homogeneous medium). For inhomogeneous media (e.g. a dielectric substrate, or finite size particles with dielectric or magnetic parameters different for those of free space) FMM can still be used as a fast matrix-vector multiplication algorithm imbedded in an iterative process for the unknown distribution of volume sources. However, the benefits of FMM in this case are much less clear. An even stronger case in favor of difference schemes (as compared to FMM) can be made if the problem is nonlinear (for example, the Poisson-Boltzmann equation).

In addition to multiparticle simulations, FLAME techniques can be applied to a variety of other problems. As a peculiar example, super high-order 3-point schemes are derived for the 1D Schrödinger equation in Section VI.F. With the 20<sup>th</sup>-order 3-point scheme as an illustration, the solution of the harmonic oscillator problem is found almost to machine precision with 10-20 grid nodes. The system matrix remains tridiagonal. Other examples include the electrostatic equation and a singular equation in 1D, 2D and 3D Collatz “Mehrstellen” schemes, electrostatic interactions of particles, scattering from dielectric cylinders, wave propagation in a photonic crystal, and plasmon resonances.

Methodologically, the main new feature of FLAME is the systematic use of local approximation spaces *in the FD context*. It is hoped that the proposed framework, with its extensive connections to many existing approaches, will stimulate further development of finite difference and finite element methods.

### III PERSPECTIVES

Development of the new class of methods can be approached from several different but related perspectives and intuitive principles.

#### A Perspective #1: Basis Functions Not Limited to Taylor Polynomials

This idea has already been discussed. Taylor polynomials are ‘generic’ and may be the best option when no *a priori* information about the solution is available. When the local behavior of the solution is known, more effective approximations can be constructed.

#### B Perspective #2: Approximating the *Solution*, Not the Equation

In classic Taylor-based FD schemes, one approximates the underlying differential equation – i.e. the operator and the right hand side. For example, on a three-point stencil in 1D, one can expect a second order approximation of the Poisson equation. There is, however, substantial redundancy built into this approach. Indeed, the scheme covers all sufficiently smooth functions for which the Taylor approximation is valid. Yet it is only the *solution* of the problem that is of direct interest; it is, in a sense, wasteful to approximate other functions.

To highlight this point, suppose for a moment that the exact solution  $u^*$  is known. It is then trivial to find a three-point scheme that is itself *exact*, e.g.:

$$u_{k-1}/u_{k-1}^* - 2u_k/u_k^* + u_{k+1}/u_{k+1}^* = 0 \quad (1)$$

It is easy to dismiss this example as frivolous, as it requires knowledge of the exact solution. The message, however, is that as more information about the solution is utilized, higher accuracy can be achieved; equation (1) is just an extreme example of this principle.

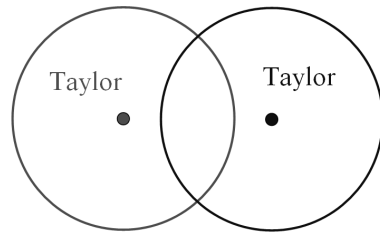


Figure 2: Taylor approximations around two grid nodes coexist in the overlap area.

A practical example is the use of *harmonic* polynomials to approximate harmonic functions (Sections VI.D, VI.E). More generally, the ‘Trefftz’ version of FLAME calculus employs basis functions that *satisfy the underlying differential equation*. No effort is wasted on trying to approximate functions that do not satisfy the equation being solved. This ‘Trefftz’ approximation is purely *local* and therefore relatively easy to construct.

#### C Perspective #3: Multivalued Approximation

In FD analysis, interpolation between the nodes is usually viewed just as a postprocessing tool not inherent in the FD method itself. However, approximation between the nodes *is* in fact an integral part of the derivation of classical FD schemes. Indeed, this approximation involves Taylor expansions around grid nodes (Fig. 2). Each of these expansions ‘lives’ in a neighborhood of its node. The disparate Taylor expansions *coexist* in the overlap region of two or more such neighborhoods. This is precisely the viewpoint taken in FLAME, except that any desirable approximating functions are allowed rather than just the Taylor polynomials. Each of these approximations is purely local and valid in the vicinity of a given grid stencil; as in FD, two or more of such approximations may coexist at any given point. The discrepancies between these approximations are expected to tend to zero if the method converges as the grid is refined. At the same time, these discrepancies may prove useful as an *a posteriori* error indicator.

#### D Perspective #4: Conformity vs. Flexibility

The following very schematic chart (Fig. 3) puts various methods into a “flexibility vs. conformity” perspective. The dashed arrow shows the general trend: flexibility of approximation can be gained by giving up some conformity of the method. Two methods stand out of that trend: GFEM and classic FD.

GFEM *outperforms* the trend: it is fully conforming (i.e. operating in a globally defined subspace of the relevant Sobolev space) and yet allows any desirable approximating functions to be used. However, this advantage is achieved at a high computational and algorithmic cost. Classic FD schemes *underperform* relative to the general trend: they are fully nonconforming and yet make use only of local polynomial (i.e. Taylor) expansions.

FLAME schemes fill the existing void in the upper-left corner of the chart: they are fully nonconforming and admit arbitrary approximations.

Clearly, it would be somewhat simplistic to ask which side of this chart is “better”. No one would question the tremendous success of conventional FE analysis lying at the ‘conformal’ end. However, the conformity requirements do impose significant limitations in many practical cases. This was understood early on in the development of FEM – hence the notion of ‘variational crimes’ [86], the Crouzeix-Raviart elements [23], etc. The

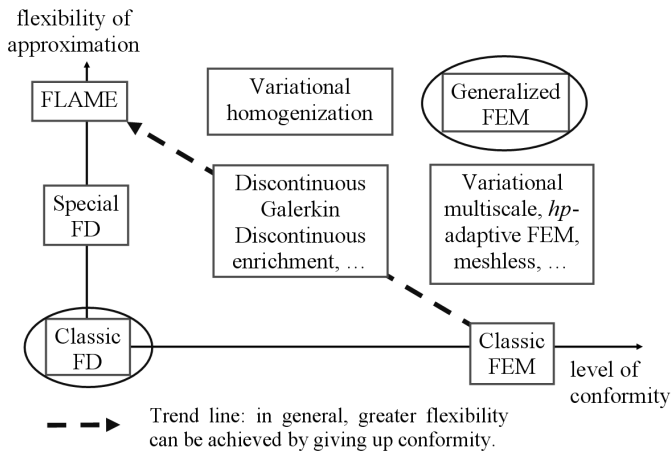


Figure 3: A schematic “conformity vs. flexibility” view of various numerical methods. One can gain flexibility of approximation by giving up conformity. This general trend is indicated by the dashed arrow. GFEM *outperforms* this trend, at a high computational and algorithmic cost. Classic FD schemes *underperform*. FLAME schemes fill the existing void.

advantages of the *nonconforming* end of the spectrum are particularly clear for problems with multiple moving particles, where finite element mesh generation may be inefficient or impractical.

#### IV AN OVERVIEW OF EXISTING METHODS FEATURING FLEXIBLE OR NONSTANDARD APPROXIMATION

##### A Disclaimer

This overview of methods related to FLAME is definitely not exhaustive and reflects not only the objective value of the methods but also their influence on the development of FLAME. Even though all the methods reviewed below share some level of “flexible approximation” as one of their features, the term “Flexible Local Approximation Methods” (FLAME) will in this paper refer exclusively to the new difference scheme developed in Section V. The new FLAME schemes are not intended to absorb or supplant any of the methods reviewed in the following subsections. These other methods, while related to FLAME, are not, generally speaking, its particular cases; nor is FLAME a particular case of any of these methods.

##### B Generalized FEM by Partition of Unity

In the Generalized FEM [65], [5], [30] [87], [6], [77], [76], [7], [29] the computational domain is covered by overlapping subdomains (“patches”). The solution is approximated locally over each patch. These individual local approximations are independent of one another and are merged by Partition of Unity (PU). The global approximation error is guaranteed to be bounded by the local (patch-wise) errors [5], [87], [6]. Strouboulis *et al.* [87] present an extensive set of application examples with special functions for material inclusions in stress analysis. Babuška *et al.* [4] apply GFEM (still at the early stages of development in 1994) to problems with material interfaces. Plaks *et al.* [76] implemented GFEM for problems with magnetized particles.

The main advantage of GFEM is that the approximating functions can in principle be arbitrary; thus GFEM definitely qualifies as a method with the kind of flexible local approximation we seek. However, there is a high algorithmic and computational

price to be paid for all the flexibility that GFEM provides. Multiplication by the partition of unity functions makes the system of approximating functions more complicated, and possibly ill-conditioned or even linearly dependent [5]. The computation of gradients and implementation of the Dirichlet conditions also get more complicated. In addition, GFEM-PU may lead to a combinatorial increase in the number of degrees of freedom [76], [92]. An even greater difficulty in GFEM-PU is the high cost of the Galerkin quadratures that need to be computed numerically in geometrically complex 3D regions (intersections of overlapping patches).

##### C Variational Homogenization

Moskow *et al.* [69] improve the approximation of the electrostatic potential near slanted boundaries and narrow sheets on regular Cartesian grids by employing special approximating functions constructed by a coordinate mapping [4]. Within each grid cell, the authors seek a tensor representation of the material parameter such that the discrete and continuous energy inner products are the same over the chosen discrete space. The overall construction in [69] relies on a special partitioning of the grid (“red-black” numbering, or the “Lebedev grid”) and on a specific, central difference, representation of the gradient. As shown in [92], this variational homogenization can be interpreted as a Galerkin method in a broken Sobolev space.

The variational version of FLAME that was previously described in [91] can be viewed as an extension of the variational-difference approach of [69] – the special ‘Lebedev’ grids and the specific approximation of gradients by central differences adopted in [69] turn out not to be really essential for the algorithm [92].

##### D Pseudospectral Methods

In pseudospectral methods (PSM) [12], [27], [73], [74], numerical solution is sought as a series expansion in terms of Fourier harmonics, Chebyshev polynomials, etc. The expansion coefficients are found by collocating the differential equation on a chosen set of grid nodes.

Typically the series is treated as *global* – over the whole domain or large subdomains. There is, however, a great variety of versions of pseudospectral methods, some of which (“spectral elements”) deal with more localized approximations and in fact overlap with the *hp*-version of FEM [66].

The key advantage of PSM is their exponential convergence, provided that the solution is quite smooth over the whole domain.

One major difficulty is the treatment of complex geometries. In relatively simple cases this can be accomplished by a global mapping to a reference shape (square in 2D or cube in 3D) but in general may not be possible. Another alternative is to subdivide the domain and use spectral elements (with ‘spectral’ approximation within the elements but lower order smoothness across their boundaries); however, convergence is then algebraic, not exponential, with respect to the parameter of that subdivision.

The presence of material interfaces is an even more serious problem, as the solution then is no longer smooth enough to yield the exponential convergence of the global series expansion.

An additional disadvantage of PSM is that the resultant systems of equations tend to have much higher condition numbers than the respective FD or FE systems [70]. This is due to the very uneven spacing of the Chebyshev or Legendre collocation

nodes typically used in PSM. Ill-conditioning may lead to accuracy loss in general and to stability problems in time-stepping procedures.

PSM have been very extensively studied over the last 30 years, and quite a number of approaches alleviating the above disadvantages have been proposed [27], [66], [70], [73]. Nevertheless it would be fair to say that these disadvantages are inherent in the method and impede its application to problems with complex geometries and material interfaces.

## E Meshless Methods

In a large variety of meshless methods – see [9], [8], [22], [24], [55], [57], [6], the prevailing technique is the Moving Least Squares (MLS) approximation. Consider a ‘meshless’ set of nodes (that is, nodes selected at arbitrary positions  $r_i$ ,  $i = 1, 2, \dots, n$ ) in the computational domain. For each node  $i$ , a smooth weighting function  $W_i(r)$  with a compact support is introduced; this function would typically be normalized to one at node  $i$  (i.e. at  $r = r_i$ ) and decay to zero away from that node. Intuitively, the support of the weighting function defines the “zone of influence” for each node.

Let  $u$  be a smooth function that we wish to approximate by MLS. For any given point  $r_0$ , one considers a linear combination of a given set of  $m$  basis functions  $\psi_\alpha(r)$  (almost always polynomials in the MLS framework):  $u_h^{(i)} = \sum_{\alpha=1}^m c_\alpha(r_0)\psi_\alpha(r)$ . Note that the coefficients  $c$  depend on  $r_0$ . They are chosen to approximate the nodal values of  $u$ , i.e. the Euclidean vector  $\{u(r_i)\}$ , in the least-squares sense with respect to the weighted norm with the weights  $W_i(r_0)$ . This least-squares problem can be solved in a standard fashion; note that it involves only nodes containing  $r_0$  within their respective “zones of influence” – in other words, only nodes  $i$  for which  $W_i(r_0) \neq 0$ .

Duarte and Oden [29] showed that this procedure can be recast as a partition of unity method, where the PU functions are defined by the weighting functions  $W$  as well as the (polynomial) basis set  $\{\psi\}$ . This leads to more general adaptive “*hp*-cloud” methods.

The trade-off for avoiding complex mesh generation is the increased computational and algorithmic complexity. The expressions for the approximating functions obtained by least squares are rather complicated [8], [24], [55], [57], [6]. The *derivatives* of these functions are even more involved. These derivatives are part of the integrand in the Galerkin inner product, and the computation of numerical quadratures is a bottleneck in meshless methods. Other difficulties include the treatment of Dirichlet conditions and interface conditions across material boundaries [22], [24], [55], [57], [48].

In the Compumag community, meshless methods were applied to electromagnetic field computation by Maréchal *et al.* [60], [59], [48].

## F Discontinuous Galerkin Methods

Discontinuous Galerkin methods (DGM) [3], [11], [15], [18], [72] relax the conformity requirements of the standard FEM. A consolidated view of DGM with extensive bibliography is presented in [3]. Many of the approaches start with the “mixed” formulation that includes additional unknown functions for the fluxes on element edges (2D) or faces (3D). However, these additional unknowns can be replaced with their numerical approximations, thereby producing a “primal” variational formulation in terms of the scalar potential alone. In DGM, the interelement continuity is ensured, at least in the weak sense, by retaining the

surface integrals of the jumps, generally leading to saddle-point problems even if the original equation is elliptic.

In electromagnetic field computation, DGM was applied by Alotto *et al.* to moving meshes in the air gap of machines [2].

## G Treatment of Material Interfaces in Finite Difference – Time Domain Methods

Finite Difference Time Domain (FDTD) methods and Finite Integration Techniques (FIT) [17], [80] require very extensive computational work due to a large number of time steps and large meshes. Therefore simple Cartesian grids are strongly preferred and the need to avoid ‘staircase’ approximations of curved or slanted boundaries is quite acute. Due to the wave nature of the problem, any local numerical error, including the errors due to the staircase effect, tend to propagate in space and time and pollute the solution overall.

A great variety of approaches to reduce or eliminate the staircase effect in FDTD have been proposed, including changes in the time-stepping formulas for the magnetic field or heuristic homogenization of material parameters based on volume or edge length ratios [26], [88], [105]. In some cases, the second order of the FDTD scheme is maintained by including additional geometric parameters or by using partially filled cells, as done by Zagorodnov *et al.* [106].

The literature on FDTD is so vast that a detailed review would not be reasonable here; please see the comprehensive database [1], monographs [88], [75] and reviews [101] for further information.

## H Special FD Schemes

Many difference schemes rely on special approximation techniques to improve the numerical accuracy. These special techniques are too numerous to list, and only the ones that are closely related to the ideas of this paper are briefly reviewed below.

For some 1D equations, Mickens [67] constructed “exact” FD schemes – that is, schemes with zero consistency error. He then developed a wider class of “nonstandard” schemes by modifying finite difference approximations of derivatives. These modified approximations are *asymptotically* (as the mesh size tends to zero) equivalent to the standard ones but for finite mesh sizes may yield higher accuracy. Similar ideas were used by Harari & Turkel [45] and by Singer & Turkel [83] to construct exact and high-order schemes for the Helmholtz equation. Cole [19], [20] applied nonstandard methods to electromagnetic wave propagation problems (high-order schemes) in 2D and 3D.

The “immersed surface” methodology [100] generalizes the Taylor expansions to account for derivative jumps at material boundaries but leads to rather unwieldy expressions.

Nehrbass [71] and Lambe *et al.* [56] modified the central coefficient of the standard FD scheme for the Helmholtz equation to minimize, in some sense, the average consistency error over plane waves propagating in all possible directions. Some similarity between the Nehrbass schemes and FLAME will become obvious in Section V. However, the derivation of the Nehrbass schemes requires very elaborate symbolic algebra coding, as the averaging over all directions of propagation leads to integrals that are quite involved. In contrast, FLAME schemes are inexpensive and easy to construct.

Very closely related to the material of the present paper are the special difference schemes developed by Hadley [42], [43], [99] for electromagnetic wave propagation. In fact, these schemes are

direct particular cases of FLAME, with Bessel functions forming a Trefftz-FLAME basis (although Hadley derives them from different considerations).

For unbounded domains, an artificial truncating boundary has to be introduced in FD and FE methods. The exact conditions at this boundary are nonlocal; however, local approximations are desirable to maintain the sparsity of the system matrix. One such approximation that has gained some popularity is the so called "Measured Equation of Invariance" (MEI) by Mei *et al.* [63], [35], [47]. As it happens, MEI can be viewed as a particular case of Trefftz-FLAME, with the basis functions taken as potentials due to some test distributions of sources.

## I Special Finite Elements

The treatment of singularities was historically one of the first cases where special approximating functions were used in the FE context – by Fix, Gulati and Wakoff in 1973 [32]. In problems of solid mechanics, Jirousek in the 1970s [52], [51] proposed ‘Trefftz’ elements, with basis functions satisfying the underlying differential equation exactly. This not only improves the numerical accuracy substantially, but also reduces the Galerkin volume integrals in the the computation of stiffness matrices to surface integrals (via integration by parts). Since then, Trefftz elements have been developed quite extensively; see a detailed study by Herrera [49] and a review paper by Jirousek & Zielinski [53].

Also in solid mechanics, Soh & Long [85] proposed two 2D elements with circular holes, while Meguid & Zhu [62] developed special elements for the treatment of inclusions.

In the method of Residual-Free Bubbles by Brezzi, Franca & Russo [13], the standard element space is also enriched with ‘Trefftz’ functions. The conformity of the method is maintained by having the bubbles vanish at the interelement boundaries. Similar ‘bubbles’ are common in hierarchical finite element algorithms (see e.g. Yserentant [104]); however, traditional FE methods – hierarchical or not – are built exclusively on piecewise-polynomial bases.

Farhat, Harari & Franca [31] relax the conformity conditions and get higher flexibility of approximation in return. As in the case of residual-free bubbles, functions satisfying the differential equation are added to the FE basis. However, the continuity at interelement boundaries is only weakly enforced via Lagrange multipliers.

In electromagnetic analysis, Trefftz expansions were used by Gyimesi *et al.* in unbounded domains [40], [41].

## V TREFFTZ-FLAME SCHEMES WITH FLEXIBLE LOCAL APPROXIMATION

### A The Model Problem

The *variational* version of FLAME was described in [91], [92]. The general setup is reviewed here for completeness. Although the potential application areas of FLAME are broad, for illustrative purposes in this section we shall have in mind the model static Dirichlet problem

$$Lu \equiv -\nabla\sigma\nabla u = f \text{ in } \Omega \subset R^n, (n = 2, 3); \quad u|_{\partial\Omega} = 0 \quad (2)$$

Here  $\sigma$  is a material parameter (conductivity, permittivity, permeability, etc.) that can be discontinuous across material boundaries and can depend on coordinates but not, in the linear case under consideration, on the potential  $u$ . The computational domain  $\Omega$  is either two- or three-dimensional. At any material in-

terface boundary  $\Gamma$ , the usual potential and flux continuity conditions hold.

### B Overlapping patches

The first ingredient of the proposed setup is the same as in GFEM: a set of overlapping patches  $\Omega^{(i)}$  covering the computational domain  $\Omega = \cup\Omega^{(i)}$ ,  $i = 1, 2, \dots, n$ . Within each patch, there is a local approximation space

$$\Psi^{(i)} = \text{span}\{\psi_\alpha^{(i)}, \alpha = 1, 2, \dots, m^{(i)}\} \quad (3)$$

Note that no *global* approximation space will be considered. Rather, the following notion is introduced:

For a given domain cover  $\{\cup\Omega^{(i)}\}$  with corresponding local spaces  $\Psi^{(i)}$ , a *multivalued approximation*  $u_h\{\cup\Omega^{(i)}\}$  of a given potential  $u$  is just a collection of patch-wise approximations:

$$u_h\{\cup\Omega^{(i)}\} \equiv \{u_h^{(i)} \in \Psi^{(i)}\} \quad (4)$$

In regions where two or more patches overlap (Fig. 4), several local approximations coexist and do not have to be the same (see Section III).

The second ingredient is a set of  $n$  nodes (the number of nodes is equal to the number of patches). Although a meshless setup is possible, we shall for maximum simplicity assume a regular grid with a mesh size  $h$ . The  $i$ -th stencil is defined as a set of  $M^{(i)}$  nodes within  $\Omega^{(i)}$ :  $\text{Stencil}^{(i)} \equiv \{\text{nodes} \in \Omega^{(i)}\}$ . For any continuous potential  $u$ ,  $\mathcal{N}u$  will denote the set of its values at all grid nodes (viewed as a Euclidean vector in  $R^n$ ), and  $\mathcal{N}^{(i)}u$  – the set of nodal values on  $\text{Stencil}^{(i)}$ . Within each patch, the

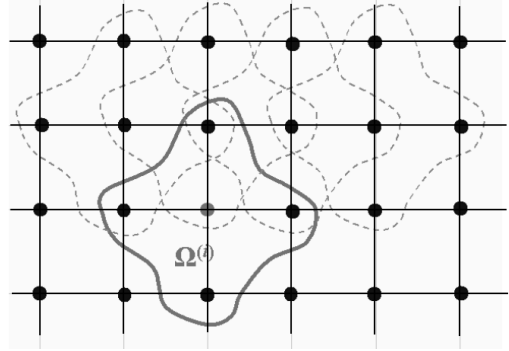


Figure 4: Overlapping patches with 5-point stencils.

approximate solution  $u_h^{(i)}$  is sought as a linear combination of  $m^{(i)}$  basis functions  $\{\psi_\alpha^{(i)}\}$ :

$$u_h^{(i)} = \sum_{\alpha=1}^{m^{(i)}} c_\alpha^{(i)} \psi_\alpha^{(i)} \quad (5)$$

One needs to relate the coefficient vector  $\underline{c}^{(i)} \equiv \{c_\alpha^{(i)}\} \in R^m$  of expansion (5) to the vector  $\underline{u}^{(i)} \in R^M$  of the nodal values of  $u_h^{(i)}$  on  $\text{Stencil}^{(i)}$ . (Both  $M$  and  $m$  can be different for different patches ( $i$ ); this is understood but not explicitly indicated for simplicity of notation.) The relevant transformation matrix  $N^{(i)}$ ,

$$\underline{u}^{(i)} = N^{(i)}\underline{c}^{(i)} \quad (6)$$

contains the nodal values of the basis functions on the stencil; if  $r_k$  is the position vector of node  $k$ , then

$$N^{(i)} = \begin{pmatrix} \psi_1^{(i)}(r_1) & \psi_2^{(i)}(r_1) & \dots & \psi_m^{(i)}(r_1) \\ \psi_1^{(i)}(r_2) & \psi_2^{(i)}(r_2) & \dots & \psi_m^{(i)}(r_2) \\ \dots & \dots & \dots & \dots \\ \psi_1^{(i)}(r_M) & \psi_2^{(i)}(r_M) & \dots & \psi_m^{(i)}(r_M) \end{pmatrix} \quad (7)$$

## C Construction of Trefftz-FLAME Schemes

Let us initially assume that the underlying differential equation within a patch  $\Omega^{(i)}$  is homogeneous:

$$Lu = 0 \quad \text{in } \Omega^{(i)} \quad (8)$$

In the remainder, we shall exclusively consider *Trefftz* methods, where the approximating functions  $\psi^{(i)}$  satisfy the underlying differential equation (8) exactly. Trefftz methods are well known in the variational context [49]; in contrast, here a purely *finite-difference* approach is taken and will prove to be attractive in a variety of cases.<sup>1</sup>

Since the basis functions by construction already satisfy the underlying differential equation, so does the approximate solution  $u_h^{(i)}$ , automatically. As we shall see, there will typically be fewer approximating functions than nodes within the patch – most frequently,  $m$  functions for  $M = m + 1$  stencil nodes. The nodal matrix  $N^{(i)}$  is thus in general rectangular.

In the simplest illustrative 1D example, with  $m = 2$  functions  $\psi_{1,2}$  at three grid points  $x_{i-1}, x_i, x_{i+1}$ , matrix  $N^{(i)}$  is

$$N^{(i)} = \begin{pmatrix} \psi_1(x_{i-1}) & \psi_2(x_{i-1}) \\ \psi_1(x_i) & \psi_2(x_i) \\ \psi_1(x_{i+1}) & \psi_2(x_{i+1}) \end{pmatrix} \quad (9)$$

Since there are only two independent parameters (coefficients in the linear combination of  $\psi_{1,2}$ ), the three nodal values on the stencil must be linearly related:  $s_{-1}u_{i-1} + s_0u_i + s_{+1}u_{i+1} = 0$  for some coefficients  $s_0, s_{\pm 1}$ . More generally for an  $M$ -point stencil, a vector of coefficients  $\underline{s}^{(i)} \in R^M$  of the difference scheme is sought to yield

$$\underline{s}^{(i)T} \underline{u}^{(i)} = 0 \quad (10)$$

for the nodal values  $\underline{u}^{(i)}$  of any function  $u_h^{(i)}$  of form (5). Due to (6) and (10),

$$\underline{s}^{(i)T} N^{(i)} \underline{c}^{(i)} = 0 \quad (11)$$

For this to hold for any set of coefficients  $\underline{c}^{(i)}$ , one must have

$$\underline{s}^{(i)} \in \text{Null}(N^{(i)T}) \quad (12)$$

If the null space is of dimension one,  $\underline{s}^{(i)}$  represents the desired scheme (up to an arbitrary factor), and (12) is the principal expression of this Trefftz-FLAME scheme. The meaning of (12) is quite simple: each equation in the system  $N^{(i)T} \underline{s}^{(i)} = 0$  implies that the respective basis function satisfies the difference scheme with coefficients  $\underline{s}^{(i)}$ . There is thus an elegant duality feature between the continuous and discrete problems: any linear combination of the basis functions satisfies both the differential equation (due to the choice of the ‘Trefftz’ basis) and the difference equation with coefficients  $\underline{s}^{(i)}$ .

While there is no obvious way to determine the dimension of the null space *a priori*, for several classes of problems considered later the dimension is indeed one. If the null space is empty, the construction of the Trefftz-FLAME scheme fails, and one may want to either increase the size of the stencil or reduce the basis set. If the dimension of the null space is greater than one, there are two general options. First, the stencil and/or the basis can be changed. Second, one may use the additional freedom in the choice of the coefficients  $\underline{s}^{(i)}$  to seek an ‘optimal’ (in some sense) scheme as a linear combination of the independent

null space vectors. For example, it may be desirable to find a diagonally dominant scheme.

Once the basis and the stencil are chosen, the Trefftz-FLAME scheme is generated in a very simple way:

- Form matrix  $N^{(i)}$  of the nodal values of the basis functions.
- Find the null space of  $N^{(i)T}$ .

It is easy to show that the Trefftz-FLAME scheme defined by (12) is invariant with respect to the choice of the basis in the local space  $\Psi^{(i)} \equiv \text{span}\{\psi_\alpha^{(i)}\}$ .

The algorithm can be sketched as a ‘machine’ for generating Trefftz-FLAME schemes (Fig. 5). It should be stressed that

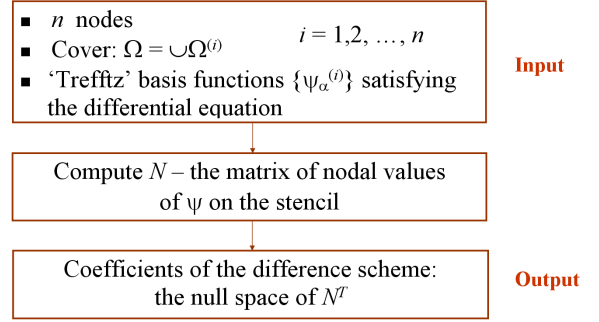


Figure 5: A ‘machine’ for Trefftz-FLAME schemes.

the algorithm is heuristic and no blanket claim of convergence can be made. The schemes need to be considered on a case-by-case basis, which is done for a variety of problems in Section V. However, consistency can be proven (Section F) in general, and convergence then follows for the subclass of schemes with a monotone difference operator [93].

## D The Treatment of Boundary Conditions

Note that in the FLAME framework approximations over different stencils are completely independent from one another. Therefore, if the domain boundary conditions are of standard types and no special behavior of the solution at the boundaries is manifest, one can simply employ any standard FD scheme at the boundary.

If the solution is known to exhibit some special features at the boundary, it may be possible to incorporate these features into the FLAME scheme. One example is Perfectly Matched Layers (PML) for electromagnetic and acoustic wave propagation considered briefly in Sections VI.K, VI.M and in some more detail in [93]. The research on FLAME-PML conditions is ongoing.

## E Trefftz-FLAME Schemes for Inhomogeneous and Nonlinear Equations

So far we considered Trefftz-FLAME schemes only for homogeneous equations (i.e. with the zero right hand side within a given patch). For inhomogeneous equations of the form

$$Lu = f \quad \text{in } \Omega^{(i)} \quad (13)$$

a natural approach is to split the solution up into a particular solution  $u_f^{(i)}$  of the inhomogeneous equation and the remainder  $u_0^{(i)}$  satisfying the homogeneous one:

$$u = u_0^{(i)} + u_f^{(i)} \quad (14)$$

<sup>1</sup>The starting point for the author’s development of Trefftz-FLAME schemes was Gary Friedman’s non-variational version of FLAME for unbounded problems [33], [44].

$$Lu_0^{(i)} = 0; \quad Lu_f^{(i)} = f \quad (15)$$

Superscript  $(i)$  emphasizes that the splitting is *local*, i.e. needs to be introduced only within its respective patch  $\Omega^{(i)}$  containing the grid stencil around node  $i$ . Since  $u_f^{(i)}$  is local (and in particular need not satisfy any exterior boundary conditions), it is usually relatively easy to construct.

Let a Trefftz-FLAME scheme  $L_h^{(i)}$  be generated for a given set of basis functions and assume that the consistency error  $\epsilon$  for this scheme tends to zero as  $h \rightarrow 0$ ; that is,

$$L_h^{(i)} \mathcal{N}^{(i)} u_0^{(i)} = \epsilon \equiv \epsilon(h, u_0^{(i)}) \rightarrow 0 \text{ as grid size } h \rightarrow 0 \quad (16)$$

where  $\mathcal{N}^{(i)}$ , as before, denotes the nodal values of a function on stencil  $(i)$ . Then clearly

$$L_h^{(i)} \mathcal{N}^{(i)} u = L_h^{(i)} \mathcal{N}^{(i)} u_0 + L_h^{(i)} \mathcal{N}^{(i)} u_f = L_h^{(i)} \mathcal{N}^{(i)} u_f + \epsilon$$

This immediately implies that the consistency error of the difference scheme

$$L_h^{(i)} \underline{u}_h = L_h^{(i)} \mathcal{N}^{(i)} u_f \quad (17)$$

is  $\epsilon$ , i.e. exactly the same as for the homogeneous case. (The Euclidean vector  $\underline{u}_h$  of nodal values does not need the superscript because the nodal values are unique and do not depend on the patch.) Note that there are absolutely no constraints on the smoothness of  $u_f^{(i)}$ , provided that its nodal values are well defined. The particular solution  $u_f^{(i)}$  can even be singular as long as the singularity point does not coincide with a grid node. For example, in [90] difference schemes of this kind were constructed for the Coulomb potential of point charges. An electrostatic problem with a line charge source is solved in a similar way in [93].

For *nonlinear* problems, the Newton-Raphson method is traditionally used for the *discrete* system of equations. In connection with FLAME schemes, Newton-Raphson-Kantorovich iterations are applied to the original continuous problem rather than the discrete one. Details are given in [93], [94].

## F Consistency of the Schemes

The consistency error of scheme (17) is, by definition, obtained by substituting the nodal values of the exact solution  $u^*$  into the difference equation. For FLAME schemes, as shown in [94], consistency follows directly from the approximation properties of the basis set. Convergence can then be proved if the scheme is monotone [94].

## VI TREFFTZ-FLAME SCHEMES: CASE STUDIES

### A The 1D Laplace Equation

The 1D Laplace equation is trivial and is used here only to fix ideas. For convenience, consider a uniform grid with size  $h$ , choose a 3-point stencil and place the origin at the middle node. Two basis functions satisfying the Laplace equation are

$$\psi_1 = 1; \quad \psi_2 = x$$

Then, since the coordinates of the stencil nodes are  $[-h, 0, h]$ , the (transposed) nodal matrix (7) is

$$N^T = \begin{pmatrix} 1 & 1 & 1 \\ -h & 0 & h \end{pmatrix}$$

and the Trefftz-FLAME difference scheme is<sup>2</sup>

$$\underline{s} = \text{Null}(N^T) = [1, -2, 1] \text{ (times an arbitrary coefficient)}$$

which coincides with the standard 3-point scheme for the Laplace equation.

### B The Helmholtz and Electrostatic Equations in 1D

A less trivial case is the 1D Helmholtz equation

$$d^2u/dx^2 - \kappa^2u = 0$$

with any complex  $\kappa$ . Let us choose the same 3-point stencil  $[-h, 0, h]$  as before and two basis functions satisfying the Helmholtz equation:

$$\psi_1 = \exp(\kappa x); \quad \psi_2 = \exp(-\kappa x)$$

Then the matrix of nodal values (7) is

$$N^T = \begin{pmatrix} \exp(-\kappa h) & 1 & \exp(\kappa h) \\ \exp(\kappa h) & 1 & \exp(-\kappa h) \end{pmatrix}$$

and the resultant difference scheme is

$$\underline{s} = \text{Null}(N^T) = [1, -2 \cosh(\kappa h), 1] \quad (18)$$

Since the theoretical solution in this 1D case is exactly representable as a linear combination of the chosen basis functions, the difference scheme *yields the exact solution* (in practice, up to the round-off error). This scheme is known and has been derived in a different way by Mickens [67] (see also Farhat *et al.* [31] and Harari & Turkel [45]).

A very similar analysis applies to the 1D linear electrostatic equation with a variable (and possibly discontinuous) permittivity  $\epsilon$ . The resultant scheme is exact (i.e. the theoretical solution satisfies the FD equation) even if  $\epsilon$  is discontinuous. The scheme has a clear interpretation as a flux balance equation [94]. Such schemes are indeed typically derived from flux balance considerations (see e.g. the ‘‘homogeneous schemes’’ in [79]) but are seen to be a natural particular case of Trefftz-FLAME.

### C The 2D and 3D Laplace Equation

Consider a regular rectangular grid, for simplicity with spacing  $h$  the same in both directions, and the standard 5-point stencil. The origin of the coordinate system is placed for convenience at the central node of the stencil. With four basis functions  $[1, x, y, x^2 - y^2]$  satisfying the Laplace equation, the nodal matrix (7) becomes

$$N^T = \begin{pmatrix} 1 & 1 & 1 & 1 & 1 \\ 0 & -h & 0 & h & 0 \\ h & 0 & 0 & 0 & -h \\ -h^2 & h^2 & 0 & h^2 & -h^2 \end{pmatrix}$$

The difference scheme is then  $\text{Null}(N^T) = [-1, -1, 4, -1, -1]$  (times an arbitrary constant), which coincides with the standard five-point scheme for the Laplace equation. A more general case with different mesh sizes in the  $x$ - and  $y$ - directions can be handled in a completely similar way.

The 3D case is fully analogous. With six basis functions  $\{1, x, y, z, x^2 - y^2, x^2 - z^2\}$  and the standard 7-point stencil on a uniform grid, one arrives, after computing the null space of the respective  $6 \times 7$  matrix  $N^T$ , at the standard 7-point scheme with the coefficients  $[-1, -1, -1, 6, -1, -1, -1]$ . As in 2D, the case of different mesh sizes in the  $x$ -,  $y$ - and  $z$ -directions does not present any difficulty.

<sup>2</sup>As a slight abuse of notation, the square-bracketed arrays (such as  $[1, -2, 1]$ ) do not distinguish between row and column vectors.

## D The Fourth Order Nine-Point Mehrstellen Scheme for the Laplace Equation in 2D

The solution is, by definition, a harmonic function. Harmonic polynomials are known to provide an excellent (in some sense, even optimal [5]) approximation of harmonic functions [5], [64]. Indeed, for a fixed polynomial order  $p$ , the FEM and harmonic approximation errors are similar [5]; however, the FEM approximation is realized in a much wider space containing *all* polynomials up to order  $p$ , not just the harmonic ones. For solving the Laplace equation, the standard FE basis set can thus be viewed as having substantial redundancy that is eliminated by using the harmonic basis.

With these observations in mind, one may choose the basis functions as harmonic polynomials in  $x, y$  up to order 4, namely,  $\{1, x, y, xy, x^2 - y^2, x(x^2 - 3y^2), y(3x^2 - y^2), (x^2 - y^2)xy, (x^2 - 2xy - y^2)(x^2 + 2xy - y^2)\}$ . Then for a  $3 \times 3$  stencil of adjacent nodes of a uniform Cartesian grid, the computation of the nodal matrix (7) (transposed) and its null space is simple with any symbolic algebra package. If the mesh size is equal in both  $x$ - and  $y$ - directions, the resultant scheme has order 6. Its coefficients are 20 for the central node,  $-4$  for the four mid-edge nodes, and  $-1$  for the four corner nodes of the stencil. In the standard texts [21], [79], this scheme is developed by manipulating the Taylor expansions for the solution and its derivatives.

## E The 4th order 19-point Mehrstellen Scheme for the Laplace Equation in 3D

Construction of the scheme is analogous to the 2D case. The 19-point stencil is obtained by considering a  $3 \times 3 \times 3$  cluster of adjacent nodes and then discarding the eight corner nodes. The basis functions are chosen as the 25 independent harmonic polynomials in  $x, y, z$  up to order 4. Computation of the matrix of nodal values (7) and of the null space of its transpose is straightforward by symbolic algebra. The resultant difference scheme is well known (it was introduced and called a ‘Mehrstellen’ scheme by Collatz [21]; see also [79]) but is typically derived from totally different considerations.<sup>3</sup> We see again that for the Laplace equation it is a natural particular case of Trefftz-FLAME. This scheme, due to its geometrically compact stencil, reduces processor communication in parallel solvers and therefore has gained popularity in computationally intensive applications of physical chemistry and quantum chemistry: electrostatic fields of multiple charges, the Poisson-Boltzmann equation in colloidal and protein simulation, and the Kohn-Sham equation of Density Functional Theory [14].

## F The 1D Schrödinger equation

This test problem is borrowed from the comparison study by Chen, Xu & Sun [16] of several FD schemes for the boundary value (rather than eigenvalue) problem for the 1D Schrödinger equation over a given interval  $[a, b]$ .

$$-u'' + (V(x) - E)u = 0, \quad u(a) = u_a, \quad u(b) = u_b \quad (19)$$

The specific numerical example is the 5<sup>th</sup> energy level of the harmonic oscillator, with  $V(x) = x^2$  and  $E = 11 (= 2 \times 5 + 1)$ . For testing and verification, boundary conditions are taken from the analytical solution, and as in [16] the interval  $[a, b]$  is  $[-2, 2]$ . The exact solution is

$$u_{\text{exact}} = (15x - 20x^3 + 4x^5) \exp(-x^2/2) \quad (20)$$

<sup>3</sup>A generalization of the Mehrstellen schemes, known as the HODIE schemes [58] (Lynch and Rice), will not be considered here.

To construct a Trefftz-FLAME scheme for (19) on a stencil  $[x_{i-1}, x_i, x_{i+1}]$  (where  $x_{i\pm 1} = x_i \pm h$ ), one would need to take two independent local solutions of the Schrödinger equation as the FLAME basis functions. The exact solution in our example is reserved exclusively for verification and error analysis. We shall construct Trefftz-FLAME scheme *pretending* that the theoretical solution is not known, as would be the case in general for an arbitrary potential  $V(x)$ .

Thus in lieu of the exact solutions the basis set will contain their approximations. Such approximations, with arbitrary degree of accuracy, can be found by Taylor expansion and lead to 3-point schemes of arbitrarily high order. For the 20<sup>th</sup>-order scheme as an example, the roundoff level is reached for the uniform grid with just 10-15 nodes (Table I). For a fixed grid size and varying order of the scheme, the error falls off very rapidly as the order is increased and quickly saturates at the roundoff level (Fig. 6).

Table I. Errors for the 3-point FLAME scheme of order 20

Number of nodes	Mean absolute error
7	2.14E-10
11	2.06E-14
15	1.75E-15

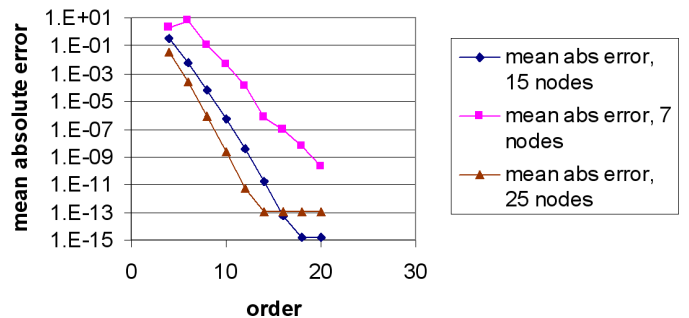


Figure 6: Error vs. order of the Trefftz-FLAME scheme for the model Schrödinger equation.

Trefftz-FLAME schemes for a 1D *singular* equation and for a time-domain equation in one spatial dimension are described in [94].

## G Line Charge Near a Slanted Boundary [93]

This problem was chosen to illustrate how FLAME schemes can rectify the notorious ‘staircase’ effect that occurs when slanted or curved boundaries are rendered on Cartesian grids. The electrostatic field is generated by a line charge located near a slanted material interface boundary between air (dielectric constant  $\epsilon = 1$ ) and water (dielectric constant  $\epsilon = 80$ ). This can be viewed as a drastically simplified 2D version of electrostatic problems in macro- and biomolecular simulation [82], [78], [36].

Four basis functions on a five-point stencil at the interface boundary were found by matching polynomial approximations in the two media via the boundary conditions. The Trefftz-FLAME result is substantially more accurate [93] than solutions obtained with the standard flux-balance scheme and with the previously used variational version of FLAME.

## H A Polarized Elliptic Particle [93]

A dielectric cylinder, with an elliptic cross-section, is immersed in a uniform external field. An analytical solution [84] is im-

posed, for testing and verification purposes, as a Dirichlet condition on the exterior boundary of the domain. The usual 5-point stencil in 2D is used.

A nonstandard feature of the Trefftz-FLAME scheme in this problem is that, four basis functions being difficult to generate, only three are used. (The first basis function is simply equal to one, and the other two correspond to the analytical solutions for the external field applied in the  $x$ - and  $y$ -directions, respectively.) This arrangement gives rise to a *two*-dimensional null space of the nodal matrix in FLAME. It then turns out to be possible to find a linear combination of the two independent difference schemes with a dominant positive diagonal entry and negative off-diagonal ones, yielding a monotone difference operator [96], [97].

## I Static Fields of Polarized or Magnetized Spherical Particles

Problems of this type arise, in particular, in the simulation of colloidal systems [28], [25]. Colloidal particles typically carry a surface electric charge giving rise to an electrostatic field. In some cases, particles can also be magnetic; controlling them by external magnetic fields may have interesting applications in some emerging areas of nanoscale assembly [102], [103], [76]. Although the equation itself is simple, computationally the problem is quite challenging due to many-body interactions and the inhomogeneities.

In a solvent without salt (or in air) the electrostatic potential is governed by the Laplace equation both inside and outside the particles, with the standard conditions at particle boundaries. The Trefftz-FLAME approximation in the vicinity of a particle is obtained with spherical harmonics:

$$u_h^{(i)} = \sum_{n=0}^{n_{\max}} \sum_{m=-n}^n P_n^m(\cos \theta) \exp(jm\phi) a_{mn} r^n$$

inside the particle, and

$$\sum_{n=0}^{n_{\max}} \sum_{m=-n}^n P_n^m(\cos \theta) \exp(jm\phi) (b_{mn} r^n + d_{mn} r^{-n-1})$$

outside the particle. The standard notation for the associated Legendre polynomials  $P_n^m$  is used. These harmonics satisfy the Laplace equation inside and outside the particle and, with a suitable choice of coefficients  $a$ ,  $b$  and  $d$ , conditions at the particle boundary (details are given in [93]). Note that the  $r^n$  term is retained outside the particle because the harmonic expansion is considered locally, in a finite (and small) patch  $\Omega^{(i)}$ .

To study convergence of Trefftz-FLAME, a classical example of a polarizable particle in a uniform external field is used. A simple analytical solution is readily available for this problem. For error analysis and verification, this analytical solution is imposed as a Dirichlet condition in the Trefftz-FLAME system.

Fig. 7 shows the relative error in the potential and field as a function of mesh size. The standard seven-point stencil is used throughout the computational domain. The observed convergence rate for the nodal values of the potential in the 2-norm is  $O(h^2)$  – i.e. the same as it would be for the identical 7-point stencil in the absence of the particle (i.e. for the Laplace equation). In other words, the presence of the particle does not degrade the performance of Trefftz-FLAME. Moreover, the field inside the particle exhibits very rapid convergence due to the fact that the approximation of the potential in and near the particle by spherical harmonics is in this example exact.

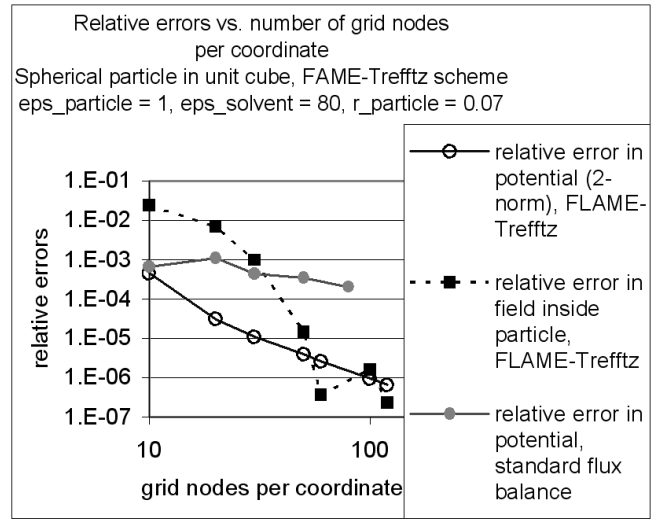


Figure 7: Superior performance of FLAME for the test problem with a polarized particle. The error in the potential is much lower than for the standard flux-balance scheme. Convergence of the field inside the particle is remarkably rapid.

## J Spherical Particles in Solvent: the Poisson-Boltzmann Equation

For monovalent salts, the potential in the solvent can be described, with a good level of accuracy, by the Poisson-Boltzmann equation (PBE):<sup>4</sup>

$$-\nabla \cdot \epsilon \nabla \phi + \kappa^2 \sinh \phi = \rho \quad (21)$$

where  $\phi$  is the normalized electrostatic potential,  $\epsilon$  is the permittivity,  $\kappa$  is the Debye–Hückel parameter and  $\rho$  is the normalized charge density of sources (macroions / particles). The hyperbolic sine term arises from the Boltzmann distribution of the microions of salt in potential  $\phi$ .

As in the previous subsection, Trefftz-FLAME basis functions can be constructed (for the linearized PBE in the Newton-Kantorovich procedure) by spherical harmonics that in this case involve spherical Bessel functions of the radius [93].

## K Scattering from a Dielectric Cylinder

In this classic example, a monochromatic plane wave impinges on a dielectric circular cylinder and gets scattered. In this Section and the following one, we consider the E-mode (one-component  $E$  field and a TM field) governed by the standard 2D equation

$$\nabla \cdot (\mu^{-1} \nabla E) + \omega^2 \epsilon E = 0 \quad (22)$$

with some radiation boundary conditions for the scattered field. The analytical solution is available via cylindrical harmonics [46] and can be used for verification and error analysis.

We consider Trefftz-FLAME schemes on a nine-point ( $3 \times 3$ ) stencil. It is natural to choose the basis functions as cylindrical harmonics in the vicinity of each particle and as plane waves away from the particles. ‘Vicinity’ is defined by an adjustable threshold:  $r \leq r_{\text{cutoff}}$ , where  $r$  is the distance from the midpoint of the stencil to the center of the nearest particle, and the threshold  $r_{\text{cutoff}}$  is typically chosen as the radius of the particle plus a few grid layers.

<sup>4</sup>For multivalent salts, the correlation effects between the ions of the salt complicate the matter.

Away from the cylinder, eight basis functions are chosen as plane waves propagating toward the central node of the nine-point stencil from each of the other eight nodes. As usual in FLAME, the  $9 \times 8$  nodal matrix  $N$  (7) of FLAME comprises the values of the chosen basis functions at the stencil nodes. The Trefftz-FLAME scheme (12) is  $\underline{s} = \text{Null}(N^T)$ . Straightforward symbolic algebra computation shows that this null space is indeed of dimension one, so that a single valid Trefftz-FLAME scheme exists. The expression for the scheme is given in [93], [94]. The scheme can be shown to be of order six with respect to the grid size.

Obviously, nodes at the domain boundary are treated differently. At the edges of the domain, the stencil is truncated in a natural way to six points: ‘ghost’ nodes outside the domain are eliminated, and the respective *incoming* plane waves associated with them are likewise eliminated from the basis set. The basis thus consists of five plane waves: three strictly outgoing and two sliding along the edge.

A similar procedure is applied at the corner nodes: a four-node stencil is obtained, and only three plane wave remain in the basis. The elimination of incoming waves from the basis thus leads, in a very natural way, to a FLAME-style Perfectly Matched Layer (PML). A detailed study of this and other versions of FLAME-PML will be reported elsewhere.

In the vicinity of the cylinder, the basis functions are chosen as cylindrical harmonics:

$$\psi_{\alpha}^{(i)} = a_n J_n(k_{\text{cyl}} r) \exp(in\phi), \quad r \leq r_0$$

$$\psi_{\alpha}^{(i)} = [b_n J_n(k_{\text{air}} r) + H_n^{(2)}(k_{\text{air}} r)] \exp(in\phi), \quad r > r_0$$

where  $J_n$  is the Bessel function,  $H_n^{(2)}$  is the Hankel function of the second kind [46], and  $a_n, b_n$  are coefficients to be determined. These coefficients are found via the standard conditions on the particle boundary; the actual expressions for these coefficients are too lengthy to be worth reproducing here but are easily usable in computer codes.

Eight basis functions are obtained by retaining the monopole harmonic ( $n = 0$ ), two harmonics of orders  $n = 1, 2, 3$  (i.e. dipole, quadrupole and octupole), and one of harmonics of order  $n = 4$ . Numerical experiments for scattering from a *single* cylinder, where the analytical solution is available for comparison and verification, show convergence (not just consistency error!) of order six for this scheme [93].

Fig. 8 shows the relative nodal error in the electric field as a function of the mesh size. Without the PML, convergence of the scheme is of the 6<sup>th</sup> order; no standard method has comparable performance. The test problem has the following parameters: the radius of the cylindrical rod is normalized to unity; its index of refraction is 4; the wavenumbers in air and the rod are one and 4, respectively. Simulations *without* the PML were run with the exact analytical value of the electric field on the outer boundary imposed as a Dirichlet condition. The field error with the PML is of course higher than with this ideal Dirichlet condition<sup>5</sup> but still only on the order of  $10^{-3}$  even when the PML is close to the scatterer (1 – 1.5 wavelengths). For the exact boundary conditions (and no PML), very high accuracy is achievable.

## L Wave Propagation in a Photonic Crystal

As a specific but consequential example, we next consider a photonic crystal analyzed by Fujisawa & Koshiba [34]. The

<sup>5</sup>It goes without saying that the exact field condition can only be imposed in test problems with known analytical solutions.

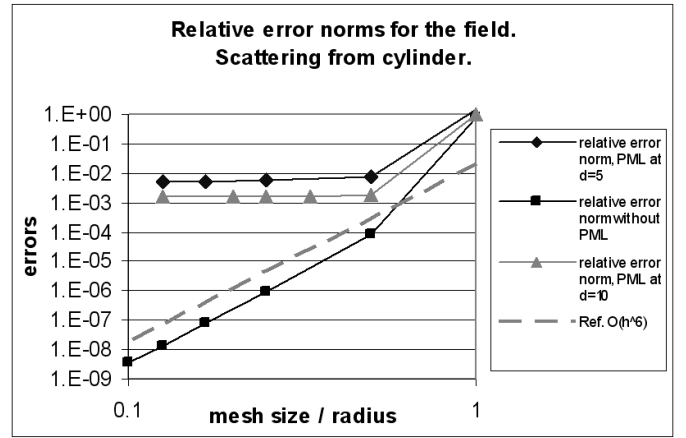


Figure 8: Relative error norms for the electric field. Scattering from a dielectric cylinder. FLAME, 9-point scheme.

waveguide with a bend is formed by eliminating a few dielectric cylindrical rods from a 2D array (Fig. 9, Fig. 10, Fig. 11)<sup>6</sup>. Fujisawa & Koshiba used a specialized finite element method to analyze time-domain beam propagation in such a waveguide, with nonlinear characteristics of the rods. The use of complex geometrically conforming finite element meshes may well be justified in this 2D case. However, regular Cartesian grids have the obvious advantage of simplicity, especially with extensions to 3D in mind. To this end, numerical experiments with FLAME schemes (as usual, operating on regular Cartesian grids) were run to test their applicability to this type of problems.

The problem is solved in the frequency domain and the material characteristic of the rods is assumed linear, with the index of refraction equal to 3. The field distribution is shown in Fig. 9.

For comparison, FE simulations (FEMLAB<sup>TM</sup>) with three meshes were run: the initial mesh with 9702 nodes, 19276 elements, and 38679 degrees of freedom (d.o.f., i.e. unknowns); a mesh obtained by global refinement of the initial one (38679 nodes, 77104 elements, 154461 d.o.f.); and an adaptively refined mesh with 27008 nodes, 53589 elements, 107604 d.o.f. The elements were 2<sup>nd</sup> order triangles in all cases. The agreement between FLAME and FEM results is excellent [93]. Fig. 10 and Fig. 11 give a visual comparison of FEM and Trefftz-FLAME meshes that provide the same accuracy level.

Note that for the  $50 \times 50$  grid there are about 10.5 points per wavelength (ppw) in the air but only 3.5 ppw in the rods, and yet the FLAME results are very accurate because of the special approximation used. Any alternative method (FE or FD) that employs generic (piecewise-polynomial) approximation would require a substantially higher number of ppw to achieve the same accuracy.

## M Coupled Plasmon Nanoparticles

**The plasmon resonance phenomenon.** The field inside a polarized particle immersed in a uniform external field can be expressed as [46], [84]

$$E = E_0 \frac{3\epsilon_p}{\epsilon_p + 2\epsilon_{\text{out}}} \quad (23)$$

where  $\epsilon_p, \epsilon_{\text{out}}$  are the dielectric constant of the particle and the surrounding medium, respectively. Other related physical quantities (the dipole moment, the polarizability, the field outside the

<sup>6</sup>The author is very grateful to Prof. Jon Webb for pointing out this example to him.

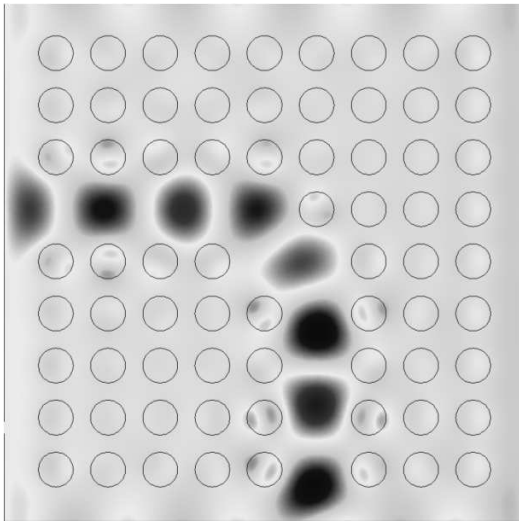


Figure 9: The imaginary part of the electric field in the photonic crystal waveguide bend.

particle) are expressed similarly and all share a singularity point at  $\epsilon_p = -2\epsilon_{out}$ . Under normal electrostatic conditions, the singu-

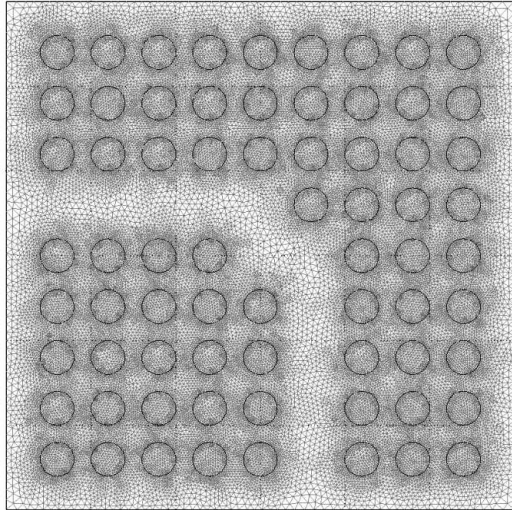


Figure 10: Finite element mesh with 38679 nodes, 77104 elements, 154461 d.o.f.

larity never manifests itself because the dielectric constants are all positive. However, in time-harmonic fields, the effective dielectric constant of materials generally becomes complex. For metals, at frequencies below the plasma frequency the effective permittivity happens to have a negative real part. This is of significant practical interest because the resonance condition (occurring at  $\epsilon_p = -2\epsilon_{out}$  for spheres, and at other negative values of  $\epsilon_p$  for other shapes) can indeed be approached. These “plasmon” resonances of nanoparticles are becoming increasingly important in applications ranging from nano-optics to nanosensors to biolabels. The high frequency case that gives rise to negative effective permittivities is, by definition, generally very far from electrostatics. However, when the particle size is very small compared to the wavelength, the electrostatic approximation is reasonable, and a strong field enhancement is indeed possible. A true singularity, though, is never obtainable, for two reasons. First, the electrostatic treatment is precise only in the limit when the particle size tends to zero relative to the wavelength; for ac-

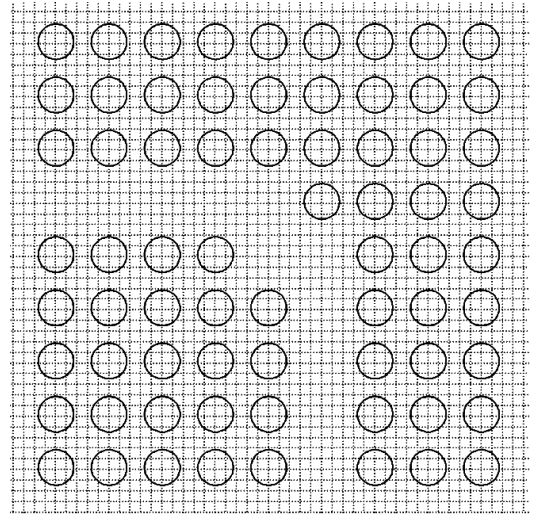


Figure 11: This  $50 \times 50$  FLAME grid (2500 d.o.f.) gives the same accuracy as the FE mesh with 154461 d.o.f.

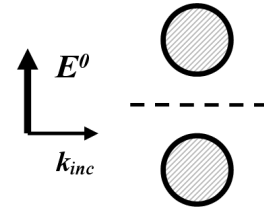


Figure 12: Two cylindrical plasmon particles. Setup due to Kottmann & Martin [54].

tual finite sizes of the particle the field enhancement is diminished due to dephasing effects. Secondly, and perhaps more importantly, the actual values of the dielectric constants are never purely real – the nonzero imaginary parts reflect the presence of losses in the material and blur the resonances.

Although the electrostatic approximation does provide a very useful insight, accurate evaluation of the resonance conditions and the field enhancement requires electromagnetic wave analysis. The governing equation for the  $H$ -mode (one-component  $H$ -field perpendicular to the computational plane and the TE-field in the plane) is

$$\nabla \cdot (\epsilon^{-1} \nabla H) + \omega^2 \mu H = 0 \quad (24)$$

The standard notation for frequency  $\omega$ , permittivity  $\epsilon$  and magnetic permeability  $\mu$  is used. In the plasmon problem, the permeability can be assumed equal to  $\mu_0$  throughout the domain; the permittivity is  $\epsilon_0$  in air and has a complex and frequency-dependent value within plasmon particles. Any standard radiation boundary conditions for the scattered wave can be used.

Note that in the  $H$ -mode (but not in the complementary  $E$ -mode) the electric field “goes through” the plasmon particles, as it does in the electrostatic limit, thereby potentially giving rise to plasmon resonances.

**Numerical results.** As an illustrative example, the following subsections describe the application of Trefftz-FLAME schemes for the problem proposed by Kottmann & Martin [54]. The physical setup involves two cylindrical plasmon particles (Fig. 12) and leads to some interesting physical effects [54]. Kottmann & Martin used integral equations in their simulation.

Nine-point Trefftz-FLAME schemes are derived in the same

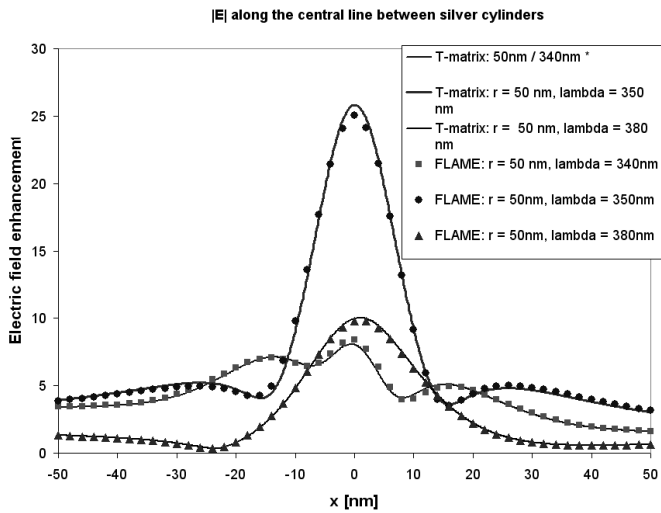


Figure 13: The magnitude of the electric field along the line connecting two silver plasmon particles. Comparison of FLAME and multipole-multicenter results. Particle radii 50 nm; varying wavelength of incident light.

way as for the scattering problem (Section K). In Fig. 13, results of the FLAME simulation are compared with the quasi-analytical solution via the multicenter-multipole expansion of the wave [95], [68].<sup>7</sup> The radius of each silver nanoparticle is 50 nm. The results of FLAME simulation are in excellent agreement with the quasi-analytical computation.

## VII DISCUSSION

The “Flexible Approximation” approach combines analytical and numerical tools: it integrates local analytical approximations of the solution into numerical schemes in a simple way. Existing applications and special cases of FLAME fall under two categories. The first one contains standard difference schemes revealed as direct particular cases of Trefftz-FLAME. The second category contains FLAME schemes that are substantially more accurate than their conventional counterparts, often with a higher rate of convergence for identical stencils. Practical implementation of Trefftz-FLAME schemes is substantially simpler than FEM matrix assembly and comparable with the implementation of conventional schemes (e.g. flux-balance schemes).

It is important to note that FLAME schemes do not have any hidden parameters to contrive better performance. The schemes are completely defined by the choice of the basis set and stencil; it is the approximating properties of the basis that have the greatest bearing on the numerical accuracy.

The collection of examples given in the paper inspires further analysis and applications of FLAME – for example, to boundary layers in eddy current problems and in semiconductor simulation (the Scharfetter-Gummel approximation [81], [33]), to varying material parameters in some protein models [36], [98], to edge and corner singularities, etc. Naturally, the author is hopeful that FLAME schemes will eventually find their use in these and other areas.

The method is most powerful when good local analytical approximations of the solution are available. For example, the advantage of the special field approximation in FLAME for the photonic crystal problem is crystal clear. Similarly, problems

<sup>7</sup>The analytical expansion was implemented by Frantisek Čajko.

with magnetizable or polarizable particles admit an accurate representation of the field around the particles in terms of spherical harmonics, and the resultant FLAME schemes are substantially more accurate than the standard control volume method.

The Trefftz-FLAME schemes are not variational, which makes their construction quite simple and sidesteps the notorious bottleneck of computing numerical quadratures. At the same time, given that this method is non-variational and especially non-Galerkin, one cannot rely on the well-established convergence theory so powerful, for example, in Finite Element analysis. For the time being, FLAME methods need to be considered on a case-by-case basis, with the existing convergence results and experimental evidence in mind. Furthermore, again because the method is non-Galerkin, the system matrix is in general not symmetric, even if the underlying continuous operator is self-adjoint. In many – but not all – cases, this shortcoming is well compensated for by the superior accuracy and rate of convergence.

FLAME schemes described in the paper use nodal values as the primary degrees of freedom (d.o.f.). Other d.o.f. could certainly be used, for example edge circulations of the field, in full analogy with edge elements and related differential-geometric treatments [10], [50], [61], [89]. The matrix of edge circulations would then be introduced instead of the matrix of nodal values in the algorithm, and the notion of the stencil would be modified accordingly.

In addition to practical usage and to the potential of generating new difference schemes in various applications, there is also some intellectual merit in having a unified perspective on different families of FD techniques such as low- and high-order Taylor-based schemes, the Mehrstellen schemes, the ‘exact’ schemes, some special schemes for electromagnetic wave propagation, the “measured equation of invariance”, and more. This unified perspective is achieved through systematic use of local approximation spaces *in the finite difference context*.

## VIII FUTURE WORK

**Short-term goals:** large-scale Trefftz-FLAME simulations of colloidal suspensions for the nonlinear Poisson-Boltzmann model, with computation of phase diagrams<sup>8</sup>; a detailed study of FLAME PML in the frequency domain; Trefftz-FLAME schemes for electromagnetic wave propagation in the time domain, for two spatial dimensions.

**Mid-term goals:** FLAME – Time Domain schemes for electromagnetic wave propagation in 3D.

**Long-term goals:** once the short- and mid-term goals have been achieved, develop a new method that will be as much fun to work with as FLAME.

## IX ACKNOWLEDGMENT

This line of research was inspired by my communication with Markus Clemens, Rolf Schuhmann and Thomas Weiland from Technische Universität Darmstadt in 2002. Another source of this research was my previous work with Alexander Plaks and Leonid Proekt on Generalized FEM. I thank Gary Friedman for many stimulating discussions and for the idea of Trefftz-FLAME methods for unbounded problems. Frantisek Čajko implemented the multipole-multicenter solutions for coupled plasmon cylinders. I thank Dmitry Golovaty and Jon Webb for reading the manuscript and suggesting numerous improvements. Finally, I

<sup>8</sup>Joint work with E. Ivanova, S. Voskoboinikov, and G. Friedman.

am grateful to the anonymous reviewers of my journal publications for their extensive and thorough reports and for numerous additional references.

## X REFERENCES

- [1] <http://www.fdttd.org>.
- [2] P. Alotto, A. Bertoni, I. Perugia, and D. Schötzau. Efficient use of the local discontinuous Galerkin method for meshes sliding on a circular boundary. *IEEE Trans. on Magnetics*, 38:405–408, 2002.
- [3] D. N. Arnold, F. Brezzi, B. Cockburn, and L. D. Marini. Unified analysis of discontinuous Galerkin methods for elliptic problems. *SIAM J. Numer. Analysis*, 39(5):1749–1779, 2002.
- [4] I. Babuška, G. Caloz, and J.E. Osborn. Special finite-element methods for a class of 2nd-order elliptic problems with rough coefficients. *SIAM J. Numer. Analysis*, 31(4):945–981, 1994.
- [5] I. Babuška and J.M. Melenk. The partition of unity method. *Int. J. for Numer. Methods in Engineering*, 40(4):727–758, 1997.
- [6] Ivo Babuška, Uday Banerjee, and John E. Osborn. Survey of meshless and generalized finite element methods: A unified approach. *Acta Numerica*, 12:1–125, 2003.
- [7] Achim Basermann and Igor Tsukerman. *Parallel generalized finite element method for magnetic multiparticle problems*, volume LNCS 3402 of *Springer Series: Lecture Notes in Computational Science and Engineering*, pages 325–339. Springer, 2005.
- [8] T. Belytschko, Y. Krongauz, D. Organ, M. Fleming, and P. Krysl. Meshless methods: an overview and recent developments. *Computer Methods in Applied Mechanics and Engineering*, 139(1–4):3–47, 1996.
- [9] T. Belytschko, Y. Y. Lu, and L. Gu. Element-free Galerkin methods. *Int. J. Numer. Meth. Engng.*, 37:229–256, 1994.
- [10] Alain Bossavit. *Computational Electromagnetism: Variational Formulations, Complementarity, Edge Elements*. San Diego: Academic Press, 1998.
- [11] C.L. Bottasso, S. Micheletti, and R. Sacco. The discontinuous Petrov-Galerkin method for elliptic problems. *Computer Methods in Applied Mechanics and Engineering*, 191(31):3391–3409, 2002.
- [12] John P. Boyd. *Chebyshev and Fourier Spectral Methods*. Publisher: Dover Publications, 2001.
- [13] F. Brezzi, L.P. Franca, and A. Russo. Further considerations on residual free bubbles for advective-diffusive equations. *Computer Methods in Applied Mechanics and Engineering*, 166:25–33, 1998.
- [14] E. L. Briggs, D.J. Sullivan, and J. Bernholc. Real-space multigrid-based approach to large-scale electronic structure calculations. *Physical Review B*, 54(20):14362–14375, 1996.
- [15] P. Castillo, B.Cockburn, I. Perugia, and D. Schötzau. An a priori error analysis of the local discontinuous Galerkin method for elliptic problems. *SIAM J. Numer. Analysis*, 38(5):1676–1706, 2000.
- [16] Rongqing Chen, Zhizhan Xu, and Lan Sun. Finite-difference scheme to solve Schrödinger equations. *Phys. Rev. E*, 47(5):3799–3802, 1993.
- [17] M. Clemens and T. Weiland. Magnetic field simulation using conformal FIT formulations. *IEEE Trans. Magn.*, 38(2):389–392, 2002.
- [18] B. Cockburn, G.E. Karniadakis, and C.-W. Shu. *The development of discontinuous Galerkin methods*, volume 11 of *Lecture Notes in Comput. Sci. Engrg.*, pages 3–50. Springer-Verlag, New York, 2000.
- [19] James B. Cole. High accuracy solution of Maxwell’s equations using nonstandard finite differences. *Computers in Physics*, 11(3):287–292, 1997.
- [20] James B. Cole. High-accuracy FDTD solution of the absorbing wave equation, and conducting Maxwell’s equations based on a nonstandard finite-difference model. *IEEE Transactions on Antennas and Propagation*, 52(3):725–729, 2004.
- [21] Lothar Collatz. *The Numerical Treatment of Differential Equations*. New York: Springer, 1966.
- [22] L. Cordes and B. Moran. Treatment of material discontinuity in the element-free Galerkin method. *Comput. Meth. Appl. Mech. Engng.*, 139:75–89, 1996.
- [23] M. Crouzeix and P.A. Raviart. Conforming and nonconforming finite element methods for solving the stationary Stokes equation. *RAIRO Anal. Numer.*, 7, R-3:33–76, 1973. MR 49:8401.
- [24] Suvranu De and Klaus-Jürgena Bathe. Towards an efficient meshless computational technique: the method of finite spheres. *Engineering Computations*, 18(1–2):170–192, 2001.
- [25] Markus Deserno, Christian Holm, and Sylvio May. Fraction of condensed counterions around a charged rod: comparison of Poisson-Boltzmann theory and computer simulations. *Macromolecules*, 33:199–205, 2000.
- [26] S. Dey and R. Mittra. A conformal finite-difference time-domain technique for modeling cylindrical dielectric resonators. *IEEE Trans. MTT*, 47(9):1737–1739, 1999.
- [27] Costas D. Dimitropoulos, Brian J. Edwards, Kyung-Sun Chae, and Antony N. Beris. Efficient pseudospectral flow simulations in moderately complex geometries. *Journal of Computational Physics*, 144:517–549, 1998.
- [28] J. Dobnikar, D. Haložan, M.Brumen, H.-H. von Grünberg, and R. Rzehak. Poisson–Boltzmann Brownian dynamics of charged colloids in suspension. *Computer Physics Communications*, 159:73–92, 2004.
- [29] C. Duarte and J. Oden. h-p adaptive method using clouds. *Comput. Meth. Appl. Mech. Engng.*, 139:237–262, 1996.
- [30] C.A. Duarte, I. Babuška, and J.T. Oden. Generalized finite element methods for three-dimensional structural mechanics problems. *Computers & Structures*, 77(2):215–232, 2000.
- [31] C. Farhat, I. Harari, and L.P. Franca. The discontinuous enrichment method. *Computer Methods in Applied Mechanics and Engineering*, 190:6455–6479, 2001.
- [32] G.J. Fix, S. Gulati, and G.I. Wakoff. On the use of singular functions with finite elements approximations. *J. Comput. Phys.*, 13:209–228, 1973.
- [33] Gary Friedman. Private communication, 2002–2005.
- [34] Takeshi Fujisawa and Masanori Koshiba. Time-domain beam propagation method for nonlinear optical propagation analysis and its application to photonic crystal circuits. *J. of Lightwave Technology*, 22(2):684–691, 2004.
- [35] Griffin K. Gothard, Sadasiva M. Rae, Tapan K. Sarkar, and Magdalena Salazar Palma. Finite element solution of open region electrostatic problems incorporating the measured equation of invariance. *IEEE Microwave and Guided Wave Letters*, 5(8):252–254, 1995.
- [36] J. A. Grant, B. T. Pickup, and A. Nicholls. A smooth permittivity function for Poisson–Boltzmann solvation methods. *J. Comp. Chem.*, 22(6):608–640, 2001. and references therein.
- [37] M. Griebel and M. A. Schweitzer. A particle-partition of unity method for the solution of elliptic, parabolic and hyperbolic PDE. *SIAM J. Sci. Comp.*, 22(3):853–890, 2000.
- [38] M. Griebel and M. A. Schweitzer. A particle-partition of unity method-part II: efficient cover construction and reliable integration. *SIAM J. Sci. Comp.*, 23(5):1655–1682, 2002.

- [39] M. Griebel and M. A. Schweitzer. A particle-partition of unity method-part III: a multilevel solver. *SIAM J. Sci. Comp.*, 24(2):377–409, 2002.
- [40] M. Gyimesi, I. Tsukerman, D. Lavers, T. Pawlak, and D. Ostergaard. Hybrid finite element-Trefftz method for open boundary analysis. *IEEE Trans. Magn.*, 32(3):671–674, 1996.
- [41] M. Gyimesi, Jian-She Wang, and D. Ostergaard. Hybrid p-element and Trefftz method for capacitance computation. *IEEE Trans. Magn.*, 37(5):3680–3683, 1996.
- [42] G. Ronald Hadley. High-accuracy finite-difference equations for dielectric waveguide analysis I: uniform regions and dielectric interfaces. *Journal of Lightwave Technology*, 20(7):1210–1218, 2002.
- [43] G. Ronald Hadley. High-accuracy finite-difference equations for dielectric waveguide analysis II: dielectric corners. *Journal of Lightwave Technology*, 20(7):1219–1231, 2002.
- [44] Derek Halverson, Gary Friedman, and Igor Tsukerman. Local approximation matching for open boundary problems. *IEEE Trans. Magn.*, 40(4):2152–2154, 2004.
- [45] I. Harari and E. Turkel. Fourth order accurate finite difference methods for time-harmonic wave propagation. *Journal of Computational Physics*, 119:252–270, 1995.
- [46] Roger F. Harrington. *Time-Harmonic Electromagnetic Fields*. Wiley-IEEE Press, 2001.
- [47] John H. Henderson and Sadasiva M. Rao. Electrostatic solution for three-dimensional arbitrarily shaped conducting bodies using finite element and measured equation of invariance. *IEEE Transactions on Antennas and Propagation*, 46(11):1660–1664, 1998.
- [48] C. Hérault and Y. Maréchal. Boundary and interface conditions in meshless methods. *IEEE Trans. Magn.*, 35:1450–1453, 1999.
- [49] Ismael Herrera. Trefftz method: A general theory. *Numer. Methods Partial Differential Eq.*, 16:561–580, 2000.
- [50] R. Hiptmair. Discrete Hodge operators. *Numer. Math.*, 90:265–289, 2001.
- [51] J. Jirousek. Basis for development of large finite elements locally satisfying all field equations. *Comp. Meth. Appl. Mech. Eng.*, 14:65–92, 1978.
- [52] J. Jirousek and N. Leon. A powerful finite element for plate bending. *Comp. Meth. Appl. Mech. Eng.*, 12:77–96, 1977.
- [53] J. Jirousek and A.P. Zielinski. Survey of Trefftz-type element formulations. *Computers & Structures*, 63:225–242, 1997.
- [54] Jörg P. Kottmann and Olivier J. F. Martin. Retardation-induced plasmon resonances in coupled nanoparticles. *Optics Letters*, 26:1096–1098, 2001.
- [55] Y. Krongauz and T. Belytschko. EFG approximation with discontinuous derivatives. *Int. J. Numer. Meth. Engng.*, 41:1215–1233, 1998.
- [56] Larry A. Lambe, Richard Luczak, and John W. Nehrass. A new finite difference method for the Helmholtz equation using symbolic computation. *International Journal of Computational Engineering Science*, 4(1):121–144, 2003.
- [57] W. Liu, S. Jun, and Y. Zhang. Reproducing kernel particle methods. *Int. J. Numer. Meth. Fluids*, 20:1081–1106, 1995.
- [58] R.E. Lynch and J.R. Rice. A high-order difference method for differential equations. *Math. Comp.*, 34:333–372, 1980.
- [59] Y. Maréchal. Some meshless methods for electromagnetic field computations. *IEEE Trans. Magn.*, 34(5):3351–3354, 1998.
- [60] Y. Maréchal, J.-L. Coulomb, G. Meunier, and G. Touzot. Use of the diffuse element method for electromagnetic field computation. *IEEE Trans. Magn.*, 29(2):1475–1478, 1993.
- [61] C. Mattiussi. An analysis of finite volume, finite element, and finite difference methods using some concepts from algebraic topology. *J. of Comp. Phys.*, 133(2):289–309, 1997.
- [62] S.A. Meguid and Z.H. Zhu. A novel finite element for treating inhomogeneous solids. *International Journal for Numerical Methods in Engineering*, 38:1579–1592, 1995.
- [63] K. K. Mei, R. Pous, Z. Chen, Y. W. Liu, and M. D. Prouty. Measured equation of invariance: A new concept in field computation. *IEEE Trans. Antennas Propagat.*, 42:320–327, 1994.
- [64] J.M. Melenk. Operator adapted spectral element methods I: harmonic and generalized harmonic polynomials. *Numer. Math.*, 84:35–69, 1999.
- [65] J.M. Melenk and I. Babuška. The partition of unity finite element method: Basic theory and applications. *Comput. Methods Appl. Mech. Engrg.*, 139:289–314, 1996.
- [66] J.M. Melenk, K. Gerdes, and C. Schwab. Fully discrete hp-finite elements: fast quadrature. *Comput. Methods Appl. Mech. Engrg.*, 190:4339–4364, 2001.
- [67] Ronald E. Mickens. *Nonstandard Finite Difference Models of Differential Equations*. Singapore; River Edge, N.J.: World Scientific, 1994.
- [68] M.I. Mishchenko, L.D. Travis, and A.A. Lacis. *Scattering, Absorption, and Emission of Light by Small Particles*. Cambridge University Press, 2002.
- [69] S. Moskow, V. Druskin, T. Habashy, P. Lee, and S. Davydycheva. A finite difference scheme for elliptic equations with rough coefficients using a Cartesian grid nonconforming to interfaces. *SIAM J. Numer. Analysis*, 36(2):442–464, 1999.
- [70] E.H. Mund. A short survey on preconditioning techniques in spectral calculations. *Applied Numerical Mathematics*, 33:61–70, 2000.
- [71] John W. Nehrass. *Advances in finite difference methods for electromagnetic modeling*. PhD thesis, Ohio State University, 1996.
- [72] J.T. Oden, I. Babuška, and C.E. Baumann. A discontinuous hp finite element method for diffusion problems. *J. of Comp. Phys.*, 146:491–519, 1998.
- [73] S.A. Orszag. Spectral methods for problems in complex geometries. *Journal of Computational Physics*, 37(1):70–92, 1980.
- [74] Richard Pasquetti and Francesca Rapetti. Spectral element methods on triangles and quadrilaterals: comparisons and applications. *Journal of Computational Physics*, 198:349–362, 2004.
- [75] Andrew F. Peterson, Scott L. Ray, and Raj Mittra. *Computational Methods for Electromagnetics*. Oxford University Press, 1998.
- [76] A. Plaks, I. Tsukerman, G. Friedman, and B. Yellen. Generalized Finite Element Method for magnetized nanoparticles. *IEEE Trans. Magn.*, 39(3):1436–1439, 2003.
- [77] L. Proekt and I. Tsukerman. Method of overlapping patches for electromagnetic computation. *IEEE Trans. Magn.*, 38(2):741–744, 2002.
- [78] W. Rocchia, E. Alexov, and B. Honig. Extending the applicability of the nonlinear Poisson–Boltzmann equation: Multiple dielectric constants and multivalent ions. *J. Phys. Chem. B*, 105(28):6507–6514, 2001.
- [79] A.A. Samarskii. *The Theory of Difference Schemes*. New York: M. Decker, 2001.
- [80] R. Schuhmann and T. Weiland. *Recent advances in finite integration technique for high frequency applications*, volume 4 of *Springer Series: Mathematics in Industry*, pages 46–57. 2004.
- [81] Siegfried Selberherr. *Analysis and Simulation of Semiconductor Devices*. Springer-Verlag, 1984.
- [82] T. Simonson. Electrostatics and dynamics of proteins. *Rep Prog Phys*, 66(5):737–787, 2003. and references therein.
- [83] I. Singer and E. Turkel. High order finite difference methods for the Helmholtz equation. *Computer Methods in Applied Mechanics and Engineering*, 163:343–358, 1998.

- [84] William B. Smythe. *Static and Dynamic Electricity*. John Benjamins Publishing Co, 1989.
- [85] A.K. Soh and Z.F. Long. Development of two-dimensional elements with a central circular hole. *Comput. Methods Appl. Mech. Engrg.*, 188:431–440, 2000.
- [86] G. Strang. *Variational crimes in the finite element method*, pages 689–710. Academic Press, New York, 1972.
- [87] T. Strouboulis, I. Babuška, and K.L. Copps. The design and analysis of the Generalized Finite Element Method. *Computer Methods in Applied Mechanics and Engineering*, 181(1–3):43–69, 2000.
- [88] Allen Taflove and Susan C. Hagness. *Computational Electrodynamics: The Finite-Difference Time-Domain Method*. Artech House Publishers, 2000.
- [89] E. Tonti. Finite formulation of electromagnetic field. *IEEE Trans. Magn.*, 38(2):333–336, 2002.
- [90] Igor Tsukerman. Efficient computation of long-range electromagnetic interactions without Fourier Transforms. *IEEE Trans. Magn.*, 40(4):2158–2160, 2004.
- [91] Igor Tsukerman. Flexible local approximation method for electro- and magnetostatics. *IEEE Trans. Magn.*, 40(2):941–944, 2004.
- [92] Igor Tsukerman. *Toward Generalized Finite Element Difference Methods for electro- and magnetostatics*, volume 4 of *Springer Series: Mathematics in Industry*, pages 58–77. 2004.
- [93] Igor Tsukerman. Electromagnetic applications of a new finite-difference calculus. *IEEE Trans. Magn.*, 41, 2005. (To appear.).
- [94] Igor Tsukerman. A class of difference schemes with flexible local approximation. *J. Comp. Phys.*, 2006. (To appear.).
- [95] Victor Twersky. Multiple scattering of radiation by an arbitrary configuration of parallel cylinders. *J. Acoust. Soc. Am.*, 24:42–46, 1952.
- [96] Richard S. Varga. *Matrix Iterative Analysis*. Berlin; New York: Springer, 2000.
- [97] V.V. Voevodin and Iu.A. Kuznetsov. *Matritsy i Vychisleniia*. Moskva: Nauka, 1984. [in Russian].
- [98] Takumi Washio. Private communication, 2002–2003.
- [99] Jon Webb. Private communication, 2004–2005.
- [100] A. Wiegmann and K.P. Bube. The explicit-jump immersed interface method: Finite difference methods for PDEs with piecewise smooth solutions. *SIAM J. Numer. Analysis*, 37(3):827–862, 2000.
- [101] K. S. Yee and Chen J.S. The finite-difference time-domain (FDTD) and the finite-volume time-domain (FVTD) methods in solving maxwell’s equations. *IEEE Trans. Antennas Prop.*, 45(3):354–363, 1997.
- [102] B. Yellen and G. Friedman. Programmable assembly of heterogeneous colloidal particle arrays. *Adv. Mater.*, 16(2):111–115, 2004.
- [103] B.B. Yellen, G. Friedman, and K.A. Barbee. Programmable self-aligning ferrofluid masks for lithographic applications. *IEEE Trans Magn.*, 40(4):2994–2996, 2004.
- [104] H. Yserentant. On the multilevel splitting of finite-element spaces. *Numerische Mathematik*, 49(4):379–412, 1986.
- [105] W. Yu and R. Mittra. A conformal finite difference time domain technique for modeling curved dielectric surfaces. *IEEE Microwave Wireless Comp. Lett.*, 11:25–27, 2001.
- [106] I.A. Zagorodnov, R. Schuhmann, and T. Weiland. A uniformly stable conformal FDTD-method in Cartesian grids. *Int. J. Numer. Model.*, 16:127–141, 2003.

#### Author’s Name and Affiliation

Igor Tsukerman  
 Department of Electrical and Computer Engineering  
 The University of Akron, OH 44325–3904, USA  
 igor@uakron.edu  
<http://www.ecgf.uakron.edu/~igor/>